

Temperature Dependence of Optical Harmonic Generation in KH_2PO_4 Ferroelectrics*

J. P. VAN DER ZIEL AND N. BLOEMBERGEN

Division of Engineering and Applied Physics, Harvard University, Cambridge, Massachusetts

(Received 24 April 1964)

Optical second-harmonic generation from KH_2PO_4 and KD_2PO_4 has been measured as a function of temperature above and below the ferroelectric transition, between 77 and 300°K. The relative values of the nonlinear constants were obtained over this temperature range. They are independent of temperature in the paraelectric phase, but change by approximately 20% at the ferroelectric transition. Second-harmonic generation from χ_{33} in the ferroelectric transition was not observed. This element is not allowed by symmetry in the paraelectric phase. An extension of the theory of nonlinear optical processes to the ferroelectric phase is discussed. Higher order tensor elements, consistent with the crystal symmetry in the paraelectric phase and the static polarization, are introduced that account for the changes in the linear and nonlinear optical susceptibilities below the transition. Single-domain crystals are necessary for the measurements in the ferroelectric phase. Multiple-domain crystals yield nonreproducible and misleading results because the domain size is comparable to the phase coherence length between the fundamental and harmonic rays. Second-harmonic generation from $\text{NH}_4\text{H}_2\text{PO}_4$ was observed from 300°K to the antiferroelectric transition point. The nonlinear constants are independent of temperature.

INTRODUCTION

THE effects of the second-order ferroelectric phase transition on the nonlinear susceptibility of KH_2PO_4 and KD_2PO_4 crystals can be investigated by measurements of the temperature dependence of the second-harmonic intensity. The refractive indices of these crystals change appreciably at the transition,¹ and it is expected that the nonlinear susceptibilities should also change at this point. Recently published measurements² appear to indicate, however, that there is no change in the second-harmonic intensity, and that there are no changes in the fundamental process of second-harmonic generation except for domain and dimensional effects. Measurements of the second-harmonic intensity under controlled conditions described in this paper lead to quantitative results which are somewhat different.

It has been customary to define the second-harmonic susceptibility of KH_2PO_4 in the paraelectric phase using a tetragonal coordinate system. Below the transition a spontaneous shear distorts this unit cell³ so that it is more convenient to use an orthorhombic cell which remains rectangular. The [100] and [010] coordinate axes of this cell are rotated 45 deg with respect to the tetragonal coordinates. For the point group symmetry C_{2v} of the ferroelectric phase³ the second-harmonic polarization is given by

$$\begin{pmatrix} P_x \\ P_y \\ P_z \end{pmatrix} = \begin{pmatrix} 0 & 0 & 0 & 0 & \chi_{15} & 0 \\ 0 & 0 & 0 & \chi_{24} & 0 & 0 \\ \chi_{32} & \chi_{31} & \chi_{33} & 0 & 0 & 0 \end{pmatrix} \begin{pmatrix} E_x^2 \\ E_y^2 \\ E_z^2 \\ 2E_y E_z \\ 2E_z E_x \\ 2E_x E_y \end{pmatrix}. \quad (1)$$

* Supported by ARPA and the Joint Services.

¹ B. Zwicker and P. Scherrer, *Helv. Phys. Acta* **17**, 346 (1944).

² R. L. Himbarger and J. L. Bjorkstam, *Appl. Phys. Letters* **3**, 109 (1963).

³ The properties of KH_2PO_4 ferroelectrics have been reviewed by W. Känzig, in *Solid State Physics*, edited by F. Seitz and D. Turnbull (Academic Press Inc., New York, 1957), Vol. 4, and F. Jona and G. Shirane, *Ferroelectric Crystals* (The Macmillan Company, New York, 1962).

For the higher D_{2d} symmetry of the paraelectric phase the additional relations $\chi_{33}=0$, $\chi_{15}=-\chi_{24}$, and $\chi_{31}=-\chi_{32}$ exist between the elements. χ_{15} and χ_{31} correspond to the χ_{14} and χ_{36} elements, respectively, defined in the tetragonal coordinate system.

The polarization is a source term in the wave equation at the second-harmonic frequency, and propagates with the phase velocity of the fundamental beam. Due to dispersion and anisotropy, the phase velocity at the second-harmonic frequency in general differs from the velocity at the fundamental. The boundary value problem of the nonlinear plane-parallel plate of thickness d has been solved in detail.^{4,5} To a good approximation, the transmitted second-harmonic intensity $S(2\omega)$ generated by the fundamental is given by

$$S(2\omega) = \hat{k} \frac{F(n^{(\omega)}, n^{(2\omega)})}{[(n^{(\omega)})^2 - (n^{(2\omega)})^2]^2} |P(2\omega)|^2 \times \sin^2[\omega c^{-1} d (n^{(\omega)} \cos\theta^{(\omega)} - n^{(2\omega)} \cos\theta^{(2\omega)})], \quad (2)$$

where $F(n^{(\omega)}, n^{(2\omega)})$ is a slowly varying function of the refractive indices $n^{(\omega)}, n^{(2\omega)}$ at the fundamental and second-harmonic frequencies, respectively. The angles $\theta^{(\omega)}$ and $\theta^{(2\omega)}$ between the platelet normal and the directions of propagation of the fundamental and second harmonic inside the crystal are related to the angle of incidence, θ_i , by⁴ $n^{(\omega)} \sin\theta^{(\omega)} = \sin\theta_i$ and $n^{(2\omega)} \sin\theta^{(2\omega)} = \sin\theta_i$. The interference of the homogeneous and inhomogeneous solutions of the wave equation causes the transmitted harmonic intensity to vary in amplitude as the angle of incidence of the laser beam is varied.

EXPERIMENTAL APPARATUS AND SAMPLE PREPARATION

A block diagram of the equipment is shown in Fig. 1. The laser ruby was cooled by conduction to liquid-

⁴ N. Bloembergen and P. S. Pershan, *Phys. Rev.* **128**, 606 (1963).

⁵ D. A. Kleinman, *Phys. Rev.* **128**, 1761 (1962).

nitrogen temperature and emitted linearly polarized light. The beam diameter was reduced by a 15-cm focal length lens to 1 mm at the position of the platelet in order to increase the area of the crystal in thermal contact with the cold finger of the sample Dewar. The cold finger could be rotated with a gear arrangement, thus varying the angle of incidence of the laser beam. By holding the laser pump power at a fixed level, and attenuating the incident beam with a series of calibrated filters, the average value of the second harmonic was found to be proportional to the square of the fundamental. In the experiment the pump power and laser intensity were held constant. The amplitudes of the fundamental and second harmonic at a constant temperature and angle of incidence varied less than 5% from pulse to pulse.

The tensor elements of Eq. (1) were measured using [010] cut platelets. With the fundamental polarized at 45 deg with respect to the [100] and [001] axes, and the second-harmonic analyzing prism oriented to transmit the beam polarized parallel to the [100] axis, the harmonic generated by χ_{15} is detected. When the static polarization is reversed in the ferroelectric phase, the [100] and [010] axes are interchanged. Harmonic generation from χ_{24} is observed in the same configuration used for χ_{15} , except that the polarization is reversed. Harmonic generation from the other tensor elements with the harmonic polarization along the [001] axis is observed by adjusting the polarization of the laser beam and the analyzing prism.

The platelets were approximately 0.6 cm long in the [100] and [001] directions and varied in thickness from 0.07 to 0.20 cm. The optical surfaces were polished flat to within 0.1 wavelength over most of the sample. Silver electrodes were evaporated on the {001} faces. These electrodes flexed with the crystal as it sheared below the transition point, while crystals coated with rigid conducting epoxy electrodes cracked at this point. To further prevent thermal shattering, the crystals were slowly cooled with an electric field of 5 to 10 kV/cm. applied. Due to the large value of the piezoelectric constant d_{36} above the transition,³ the crystals are elastically soft. Below the transition the value of

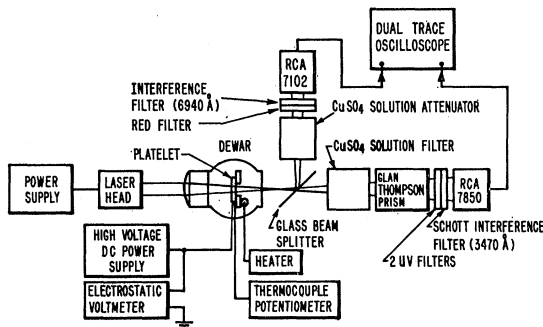


FIG. 1. Block diagram of the equipment.

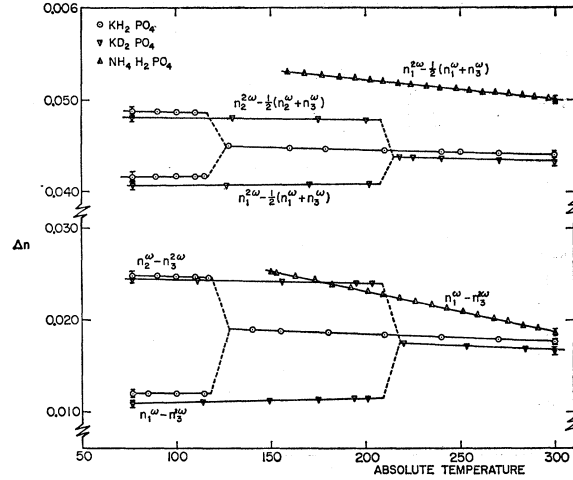


FIG. 2. The temperature dependence of the linear index mismatch corresponding to the nonlinear tensor elements of KH_2PO_4 , KD_2PO_4 , and $\text{NH}_4\text{H}_2\text{PO}_4$.

d_{36} decreases with increasing polarization and the crystals become hard again.

EXPERIMENTAL RESULTS

The differences between the refractive indices of the fundamental and second-harmonic waves must be known accurately in order to evaluate the relative values of the nonlinear constants from the second-harmonic intensity. The differences in the refractive indices are most easily obtained using the method of Maker *et al.*⁶ by observing the oscillatory dependence of the second-harmonic intensity on the angle of incidence of the laser beam with respect to the normal surface of the platelet [Eq. (2)]. The condition of index matching first used by Giordmaine⁷ and Marker *et al.*⁶ was avoided in this experiment. Near the index matched direction the second-harmonic intensity depends critically on the spatial structure of the laser beam. This is less important far from the matched direction. We discuss here the calculation of the index mismatch for KH_2PO_4 in the para- and ferroelectric phases.

The refractive indices of a wave propagating in a direction \mathbf{s} in a biaxial crystal are obtained from the solution of Fresnel's equation of the wave normals

$$\sum_{i=1}^3 s_i^2 (n^2 - n_i^2)^{-1} = 0, \quad (3)$$

where n_i is the refractive index for a wave polarized parallel to the i th Cartesian coordinate.⁸ The two refractive indices for waves propagating in the plane

⁶ P. D. Maker, R. W. Terhune, M. Nisenoff, and C. M. Savage, *Phys. Rev. Letters* **8**, 21 (1962).

⁷ J. A. Giordmaine, *Phys. Rev. Letters* **8**, 19 (1962).

⁸ M. Born and E. Wolf, *Principles of Optics* (Pergamon Press, Ltd., London, 1959), p. 662.

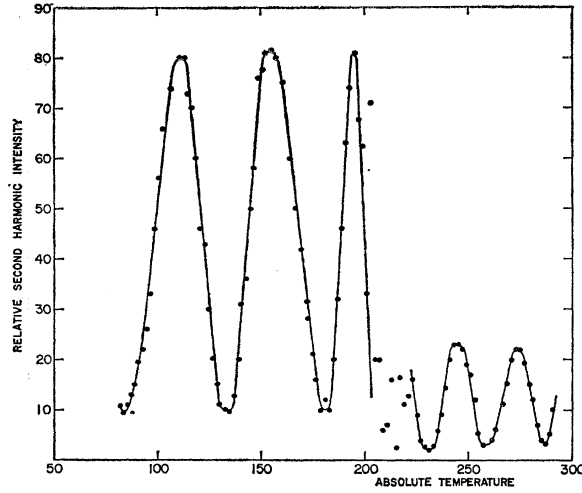


FIG. 3. The temperature dependence of the second-harmonic intensity generated by χ_{31} from a 0.1808-cm-thick KD_2PO_4 platelet.

perpendicular to the $[001]$ axis are

$$n^2 = n_3^2, \quad (4a)$$

$$n^{-2} = n_1^{-2} \cos^2\theta + n_2^{-2} \sin^2\theta, \quad (4b)$$

where θ is the angle between the direction of propagation and the $[010]$ axis. Equations (4a) and (4b) correspond to polarizations of the electric field vector parallel and perpendicular to the $[001]$ axis, respectively.

In the paraelectric phase, the crystals are uniaxial with $n_1 = n_2$. The sections of the normal surface in the plane perpendicular to the $[001]$ axis are 2 circles, and the index mismatch $n_1^{(\omega)} - n_3^{(2\omega)}$ corresponding to harmonic generation from χ_{31} is constant. Express $\theta^{(\omega)}$ in Eq. (2) in terms of $\theta^{(2\omega)}$, $n^{(\omega)}$, and $n^{(2\omega)}$ and expand the argument of \sin^2 in Eq. (2) in terms of the color dispersion retaining only terms linear in $n_3^{(2\omega)} - n_1^{(\omega)}$. One finds that the directions $\theta_m^{(2\omega)}$ in the crystal for minimum second-harmonic intensity are given by

$$\omega c^{-1} d(n_1^{(\omega)} - n_3^{(2\omega)}) = m\pi \cos\theta_m^{(2\omega)}, \quad (5)$$

where m is an integer. The index mismatch $n_1^{(2\omega)} - \frac{1}{2}(n_1^{(\omega)} + n_3^{(\omega)})$, associated with χ_{15} , is obtained from the intensity minima, using Eq. (5) with this quantity replacing $n_1^{(\omega)} - n_3^{(2\omega)}$.

The second-harmonic intensity from χ_{31} and χ_{15} was measured as a function of θ at 300°K for four samples of different thicknesses for both crystals. The average values of the index mismatch obtained from these measurements are indicated by the points at 300°K in Fig. 2 and are compared with the published values in Table I. The measured values are somewhat smaller than the results obtained by Miller *et al.*⁹

In the ferroelectric phase, with a single-domain

crystal, the ellipsoid of the wave normals is biaxial. The refractive indices for waves propagating perpendicular to the $[001]$ axis are given directly by Eqs. (4a) and (4b). The index mismatch cannot be obtained directly from the angles of the minimum second-harmonic intensity, as in the paraelectric case, since the index for a wave polarized in the plane of incidence is a function of the angle θ . An expression for the second-harmonic minima in terms of the index mismatch for waves polarized along the coordinate axes is obtained by expanding the argument of the sine term [Eq. (2)] and Eq. (4b) in terms of $\sin^2\theta^{(2\omega)}$ up to $\sin^4\theta^{(2\omega)}$. Higher order terms are negligible for the range of $\theta^{(2\omega)}$ used in this experiment. The equation for the minima in the second-harmonic intensity generated by χ_{31} , for a fundamental propagating near the $[010]$ axis is

$$\omega c^{-1} d\left\{ (n_1^{(\omega)} - n_3^{(2\omega)}) + \left[(n_2^{(\omega)} - n_3^{(2\omega)}) - \frac{1}{2}(n_1^{(\omega)} - n_3^{(2\omega)}) + 0\left\{ (n_2^{(\omega)}/n_3^{(2\omega)} - 1)^2 \right\} \right] \sin^2\theta_m^{(2\omega)} + (A) \sin^4\theta_m^{(2\omega)} \right\} = m\pi, \quad (6)$$

where (A) is a quantity of the same order as the coefficient of the $\sin^2\theta_m^{(2\omega)}$ term. With the fundamental propagating near the $[100]$ axis, corresponding to second-harmonic generation from χ_{32} , a similar expression for the intensity minima is obtained, but with $n_1^{(\omega)}$ and $n_2^{(\omega)}$ interchanged.

The second-harmonic intensity from χ_{31} and χ_{32} was measured as a function of θ at 77°K for the samples previously used at 300°K. There were at least 4 minima for each measurement. The coefficient of the $\sin^2\theta_m^{(2\omega)}$ term was obtained from a least-squares fit¹⁰ of the angles $\theta_m^{(2\omega)}$ to the integers m , and the average of the quantity in the square brackets was obtained for the four thicknesses. The two resulting equations, corresponding to second-harmonic generation from χ_{31} and χ_{32} , were solved simultaneously to obtain $n_1^{(\omega)} - n_3^{(2\omega)}$ and $n_2^{(\omega)} - n_3^{(2\omega)}$. A similar analysis was used to obtain the values

TABLE I. The values of the index mismatch of KH_2PO_4 , KD_2PO_4 , and $\text{NH}_4\text{H}_2\text{PO}_4$ at 300°K, obtained from the second-harmonic experiment, compared with the results of Miller *et al.* (Ref. 9) and the values obtained from the available refractive index data.

| Crystal | | Present measurement | Measurement of Miller <i>et al.</i> | From refractive index data |
|------------------------------------|--|---------------------|-------------------------------------|----------------------------|
| KH_2PO_4 | $n_1^{(\omega)} - n_3^{(2\omega)}$ | 0.0177 | 0.0187 | 0.0184 |
| | $n_1^{(2\omega)} - \frac{1}{2}(n_1^{(\omega)} + n_3^{(\omega)})$ | 0.044 | 0.0476 | 0.0482 |
| KD_2PO_4 | $n_1^{(\omega)} - n_3^{(2\omega)}$ | 0.0167 | 0.0168 | ... |
| | $n_1^{(2\omega)} - \frac{1}{2}(n_1^{(\omega)} + n_3^{(\omega)})$ | 0.0433 | 0.0450 | ... |
| $\text{NH}_4\text{H}_2\text{PO}_4$ | $n_1^{(\omega)} - n_3^{(2\omega)}$ | 0.0187 | 0.0196 | 0.0191 |
| | $n_1^{(2\omega)} - \frac{1}{2}(n_1^{(\omega)} + n_3^{(\omega)})$ | 0.050 | 0.0518 | 0.0543 |

⁹ R. C. Miller, D. A. Kleinman, and A. Savage, Phys. Rev. Letters 11, 146 (1963).

¹⁰ A. G. Worthing and J. Geffner, *Treatment of Experimental Data* (John Wiley & Sons, Inc., New York, 1943), p. 250.

of $n_1^{(\omega)} - \frac{1}{2}(n_1^{(\omega)} + n_3^{(\omega)})$ and $n_2^{(2\omega)} - \frac{1}{2}(n_2^{(\omega)} + n_3^{(\omega)})$ from the measurements of the second-harmonic intensity generated by χ_{15} and χ_{24} . The results for the two crystals are given by the points at 77°K in Fig. 2.

The second-harmonic intensity was also measured every 2°K at normal incidence as the temperature was varied from 77 to 300°K. A typical curve for the second harmonic intensity generated by χ_{31} in a 0.1808-cm-thick KD_2PO_4 platelet is shown in Fig. 3. Figure 4 gives the second-harmonic intensity generated by χ_{32} for the same sample in the same orientation with the same incident laser power, but with the polarity of the biasing field reversed. The change in the second-harmonic amplitude at the transition is evident from these curves. At 77°K, the ratio of the maximum amplitudes from χ_{31} and χ_{32} is 12.75. The slow oscillation of the second-harmonic intensity is due to the temperature

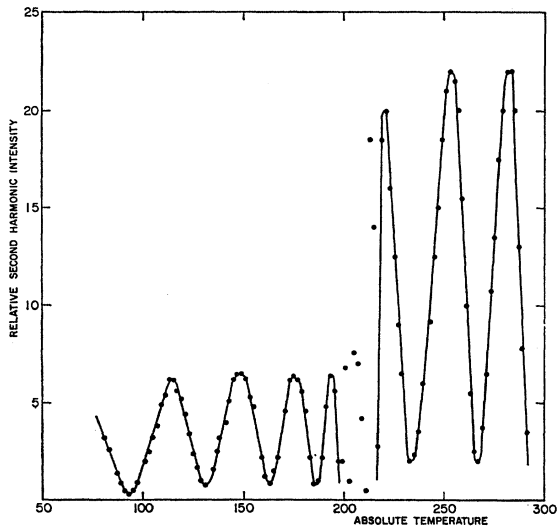


FIG. 4. The temperature dependence of the second-harmonic intensity generated by χ_{32} from the same platelet.

variation of the index mismatch. Near the transition point, the index mismatch changed too rapidly to measure the oscillations. The biasing field was reduced to zero above the transition point in order to eliminate the contribution of the electro-optic constant to the temperature dependence of the index mismatch. Below the transition point, the biasing field amplitude has no effect on the second-harmonic amplitude when the crystal was a single domain, indicating that the electro-optic constant is appreciably smaller below than above the transition point. The small changes in the index mismatch with temperature are given by the intermediate points between 77 and 300°K in Fig. 2, with the abrupt change in the mismatch near the transition point shown dotted. Near the transition temperature, the second-harmonic intensity remained within the values obtained at 77 and 300°K, and there appears to

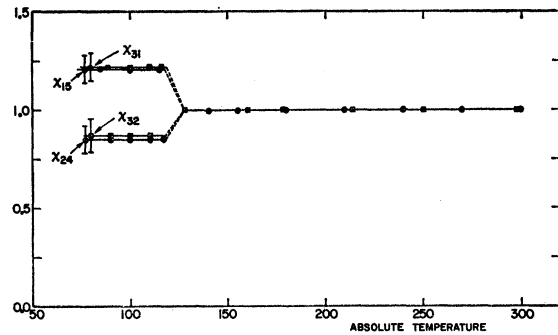


FIG. 5. The temperature dependence of the second-harmonic tensor elements of KH_2PO_4 . The ferroelectric transition temperature is 122°K.

be no change in the nonlinearity above or below this point. The relative values of the nonlinear constants were obtained from the relative amplitude measurements and the index mismatch data of Fig. 2, using Eqs. (1) and (2). The results for KH_2PO_4 are shown in Fig. 5, and for KD_2PO_4 in Fig. 6. The vertical strokes at 77°K indicate the root-mean-square deviation from the average.

Several attempts were made to observe second-harmonic generation from χ_{33} . No signals larger than the noise generated in the photomultiplier were observed. Using the index mismatch data at 300°K for the fundamental and second-harmonic polarized parallel to the [001] axis, it was determined that χ_{33} at 77°K was less than 0.03 times the value of χ_{31} at 300°K for KH_2PO_4 and KD_2PO_4 .

With a multiple-domain crystal, the oscillatory behavior of the second-harmonic intensity as a function of angle of incidence is not obtained, but a more or less random amplitude results. In some cases a second harmonic intensity 50 times larger than the maximum value at 300°K has been observed in the orientation where the second harmonic is generated by χ_{31} or χ_{32} .¹¹ Similar results were obtained for the second-harmonic

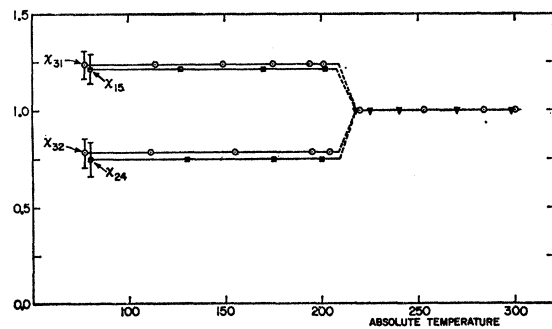


FIG. 6. The temperature dependence of the second-harmonic tensor elements of KD_2PO_4 . The ferroelectric transition temperature is 213°K.

¹¹ J. van der Ziel and N. Bloembergen, Bull. Am. Phys. Soc. 8, 380 (1963).

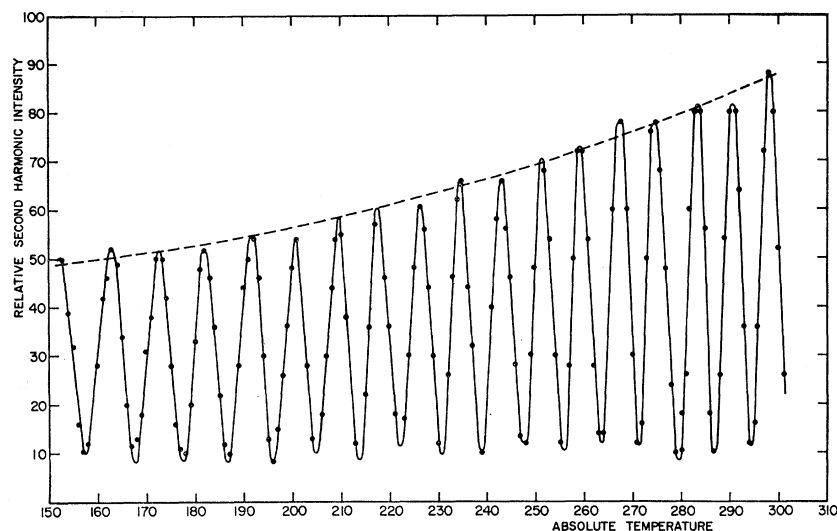


FIG. 7. The temperature dependence of the second-harmonic intensity from $\chi_{31} = -\chi_{32}$ in a 0.0932-cm-thick platelet of $\text{NH}_4\text{H}_2\text{PO}_4$. The envelope is calculated from Eq. (2).

intensity generated by χ_{15} and χ_{24} . The influence of domains was further investigated by cooling a platelet, with a field of 8 kV/cm applied, to 80°K to obtain a single domain. The coercive field of this platelet was approximately 5 kV/cm. The second-harmonic intensity generated by χ_{31} , with the regular oscillatory behavior, was observed. While monitoring the second-harmonic intensity, the biasing field was slowly reduced to zero, the polarity was reversed, and the field increased to -1 kV/cm. At this field, the second harmonic was larger than the maximum intensity obtained from χ_{31} when the crystal was a single domain. A further increase in the field caused an abrupt decrease in the second-harmonic intensity, but a further small increase in the field resulted in a large second-harmonic intensity again. The jumps in the intensity occurred when Barkhausen current signals were observed in the biasing field supply. Images observed visually through the platelet appeared unclear with this field strength. A further increase in the field appeared to clear the crystal, and the oscillatory period and the amplitude as a function of angle of incidence characteristic of χ_{32} was observed. These effects were less noticeable with low coercive field samples. Miller¹² has observed and discussed the domain effects in ferroelectric BaTiO_3 . The effects in multiple domain KH_2PO_4 are slightly complicated by the opposite signs of the nonlinear constants and the differences in the magnitudes of these constants and the index mismatches.

Depolarization effects due to domain structure were observed in the attempts to detect harmonic generation from χ_{33} . With multiple-domain crystals a second-harmonic intensity up to 0.1 of the maximum intensity from χ_{31} above the transition was observed. The second harmonic was generated by χ_{31} and χ_{32} from the fraction of the incident beam that was depolarized by the domains perpendicular to the [001] axis. These results

were not reproducible and depended on the biasing field strength.

The second-harmonic intensity generated by $\chi_{31} = -\chi_{32}$ in a 0.0932-cm-thick $\text{NH}_4\text{H}_2\text{PO}_4$ platelet as a function of temperature is shown in Fig. 7. The oscillations in the second-harmonic intensity indicate that the index mismatch changes more rapidly with temperature than in KH_2PO_4 . By first measuring the intensity as a function of θ , and then over a small temperature range at an angle of incidence midway between angles giving maximum and minimum intensity, the index mismatch was observed to increase with decreasing temperature. The temperature dependence of the index mismatch for $\text{NH}_4\text{H}_2\text{PO}_4$ corresponding to χ_{31} and χ_{15} is shown in Fig. 2. If a constant value for χ_{31} is assumed, and the known index mismatch data is used, the relative maximum intensity shown dotted in Fig. 7 is obtained as a function of temperature. Agreement between the observed and calculated peak intensities is satisfactory, indicating that χ_{31} is independent of temperature above the antiferroelectric transition point. Using a similar analysis, the element χ_{15} was also found to be independent of temperature over the range from 157 to 300°K. Barrett and Weber¹³ have measured the temperature dependence of the second-harmonic generation in KH_2PO_4 and $\text{NH}_4\text{H}_2\text{PO}_4$ above the transition temperatures to 370°K in the matched direction. They observe a linear change of the index matching angle with temperature, but did not investigate the effect of the ferroelectric phase transition on the nonlinearity.

DISCUSSION

The changes in the index mismatch below the ferroelectric transition may be compared with the temperature dependence of the birefringence measured by

¹² R. C. Miller (to be published).

¹³ J. J. Barrett and A. Weber, Phys. Rev. **131**, 1469 (1963).

TABLE II. A comparison of the difference in the refractive indices $n_1^{(\omega)} - n_2^{(\omega)}$ at 77°K.

| | Present measurement | Zwicker and Scherrer ¹ |
|--------------------------|-----------------------|-----------------------------------|
| KH_2PO_4 | 1.29×10^{-2} | 1.16×10^{-2} |
| KD_2PO_4 | 1.37×10^{-2} | 1.30×10^{-2} |

Zwicker and Scherrer.¹ In the second-harmonic experiment the difference between the refractive indices at the fundamental and second-harmonic frequencies are found. The differences between the refractive indices $n_1^{(\omega)}$ and $n_2^{(\omega)}$ at the fundamental frequency are obtained directly from Fig. 2. The present measurements and their results at 5461 Å for KH_2PO_4 and KD_2PO_4 are shown in Table II. The discrepancies are within the experimental error of the present experiment.

Zwicker and Scherrer point out that the change in $n_1^{(\omega)} - n_3^{(\omega)}$ below the ferroelectric transition may be expanded in a power series of the static polarization. Only a linear change is apparent from Fig. 2, but their more accurate measurements indicate the presence of a small contribution proportional to the square of the polarization. They further found that in the paraelectric phase the electro-optic constant r_{63} has a Curie-Weiss temperature dependence. In contrast, the electro-optic constant with the induced static polarization as the independent variable is nearly independent of temperature. By using the temperature-independent electro-optic constant of the paraelectric phase and the static polarization of the ferroelectric phase, they observe that the resulting value of the birefringence is in fair agreement with the measured values.

The general theory of nonlinear optical processes discussed by Armstrong *et al.*¹⁴ will be used to interpret these results and the changes in the second-harmonic constants below the ferroelectric transition. In their formulation, the atomic polarization is proportional to a power of the electric field acting on the atom. In dense media the appropriate local field must be used. When the local field is expressed in terms of the applied electric field, a macroscopic susceptibility is obtained consisting of the product of the microscopic susceptibility and the local field corrections for the fields and the polarization. Consider the example of a cubic crystal. The local field is

$$\mathbf{E}_{100} = \mathbf{E} + (4\pi/3)\mathbf{P}, \quad (7)$$

where \mathbf{P} is the polarization. Using the dielectric constant ϵ , \mathbf{E}_{100} in terms of \mathbf{E} is

$$\mathbf{E}_{100} = \frac{1}{3}[\epsilon + 2]\mathbf{E}. \quad (8)$$

Expressed in terms of the polarization, \mathbf{E}_{100} is

$$\mathbf{E}_{100} = (4\pi/3)[1 + 3/(\epsilon - 1)]\mathbf{P}. \quad (9)$$

The local field is proportional to the polarization when $[\epsilon - 1] \gg 3$. The true local field correction for KH_2PO_4 is undoubtedly more complicated than in this simple example, but these differences should not change this proportionality appreciably. Since ferroelectrics characteristically have large low-frequency dielectric constants, the low-frequency local field is to a good approximation proportional to the polarization.

Ward and Franken¹⁵ have shown that the electro-optic constant r_{63} is related to the nonlinear electro-optic susceptibility by

$$r_{63} = -4\pi n_0^{-4} \chi_{123}(\omega = \omega + 0). \quad (10)$$

The complete tensor index notation will henceforth be used and the frequencies of the fields associated with the indices will be included to identify the tensor elements. The Curie-Weiss temperature dependence of r_{63} thus is due to the temperature dependence of the low-frequency local field correction included in $\chi_{123}(\omega = \omega + 0)$. The nonlinear susceptibility with the polarization as variable does not include the temperature-dependent terms of the local field correction explicitly and thus is independent of temperature. Since the ultraviolet absorption does not appear to change at the transition,¹⁶ the atomic electro-optic susceptibility with absorption frequencies in the ultraviolet should be independent of temperature. The electro-optic susceptibility with the polarization as the variable then will also not change at the transition except for possible changes in the local field correction. The results of Zwicker and Scherrer indicate that the latter are small.

It is thus useful to define hybrid nonlinear susceptibilities for which the induced polarization is proportional to a product of the optical frequency electric fields and the low-frequency polarization. Higher order tensor elements are introduced which are consistent with the symmetry of the paraelectric phase, and the C_∞ symmetry of the static polarization. It is necessary to include terms proportional to the square of the polarization. In order to compare the susceptibilities with the experiment, it is convenient to transform the tensor elements to the orthorhombic coordinate frame. These elements will be denoted by primes. The relative signs of the elements in the orthorhombic frame are preserved by defining the elements in the tetragonal frame. The refractive indices are given by $n_i^2 - 1 = 4\pi\chi_{ii}'$, where the χ_{ii}' in the presence of the polarization are given by

$$\chi_{11}'(\omega) = \chi_{11}(\omega) + \chi_{123}(\omega = \omega + 0)P_3 + \chi_{1133}(\omega = \omega + 0 + 0)P_3^2, \quad (11a)$$

$$\chi_{22}'(\omega) = \chi_{11}(\omega) - \chi_{123}(\omega = \omega + 0)P_3 + \chi_{1133}(\omega = \omega + 0 + 0)P_3^2, \quad (11b)$$

$$\chi_{33}'(\omega) = \chi_{33}(\omega) + \chi_{3333}(\omega = \omega + 0 + 0)P_3^2. \quad (11c)$$

¹⁴ J. A. Armstrong, N. Bloembergen, J. Ducuing, and P. S. Pershan, Phys. Rev. **127**, 1918 (1962).

¹⁵ J. F. Ward and P. A. Franken, Phys. Rev. **133**, A183 (1964).

¹⁶ T. R. Sliker and S. R. Burlage, J. Appl. Phys. **34**, 1837 (1963).

The term $\chi_{123}(\omega=\omega+0)$ is the linear electro-optic constant and $\chi_{1133}(\omega=\omega+0+0)$ and $\chi_{3333}(\omega=\omega+0+0)$ are the quadratic electro-optic constants observed by Zwicker and Scherrer.

Similarly, the elements of the second-harmonic susceptibility in the presence of the polarization are

$$\chi_{113}'(2\omega) = +[\chi_{123}(2\omega=\omega+\omega) + \chi_{1133}(2\omega=\omega+\omega+0)P_3 + \chi_{12333}(2\omega=\omega+\omega+0+0)P_3^2], \quad (12a)$$

$$\chi_{223}'(2\omega) = -[\chi_{123}(2\omega=\omega+\omega) - \chi_{1133}(2\omega=\omega+\omega+0)P_3 + \chi_{12333}(2\omega=\omega+\omega+0+0)P_3^2], \quad (12b)$$

$$\chi_{311}'(2\omega) = +[\chi_{312}(2\omega=\omega+\omega) + \chi_{3113}(2\omega=\omega+\omega+0)P_3 + \chi_{31233}(2\omega=\omega+\omega+0+0)P_3^2], \quad (12c)$$

$$\chi_{322}'(2\omega) = -[\chi_{123}(2\omega=\omega+\omega) - \chi_{3113}(2\omega=\omega+\omega+0)P_3 + \chi_{31233}(2\omega=\omega+\omega+0+0)P_3^2], \quad (12d)$$

$$\chi_{333}'(2\omega) = \chi_{3333}(2\omega=\omega+\omega+0)P_3. \quad (12e)$$

The minus signs in Eqs. (12b) and (12d) are the result of the transformation from the tetragonal to the orthorhombic coordinate frame and since the choice of orthorhombic axes is not unique, only the relative signs are of importance. The dispersion between the fundamental and second harmonic frequencies is small for the crystals measured. The Kleinman symmetry relations¹⁷ then indicate that elements with permutations of the same indices are equal, and thus have the same sign. This permutation does not apply to indices corresponding to the static polarization.

The term linear in the polarization increases the absolute magnitude of $\chi_{311}'(2\omega)$ and decreases the complementary element $\chi_{322}'(2\omega)$ with respect to the magnitude of the nonlinearity above the transition point. The quadratic term changes the absolute magnitude of both elements in the same manner.

The experimental measurement of the second-harmonic intensity near the transition temperature was not accurate enough to make a definite statement about the dependence of the nonlinear tensor elements on the polarization. It appears from Figs. 5 and 6 that the major contribution to the change in the nonlinearity is due to the term linear in the polarization. The tensor element $\chi_{3333}(2\omega)$ is apparently small compared to $\chi_{3113}(2\omega)$.

A comparison of the tensor elements of the same rank appearing in Eqs. (11) and (12) can be made if it is assumed that dispersive effects of the susceptibilities for single atoms are negligibly small. This is equivalent to the assumption that electronic rather than ionic processes predominate, with absorption frequencies far in the ultraviolet. Lattice and ionic effects will, however, still enter through the appropriate local field corrections, introducing dispersion in the macroscopic, observed, tensor elements. One expects the following

proportionality to hold.

$$\frac{\chi_{123}(\omega=\omega+0)P_3}{\chi_{312}(2\omega=\omega+\omega)} = \frac{\chi_{1133}(\omega=\omega+0+0)P_3^2}{\chi_{3113}(2\omega=\omega+\omega+0)P_3} = \frac{\chi_{3333}(\omega=\omega+0+0)P_3^2}{\chi_{3333}(2\omega=\omega+\omega+0)P_3}. \quad (13)$$

Relations between experimentally accessible quantities occurring in Eqs. (11) and (12) have been obtained by multiplying the susceptibilities by the appropriate power of the polarization. The local field corrections implicit in the susceptibilities are the same for each ratio. This analysis is an extension of the symmetry conditions proposed by Kleinman.¹⁷

Using the n_1-n_2 data of Zwicker and Scherrer for KH_2PO_4 given in Table II results in a value of $\chi_{123}(\omega)P_3 = 1.38 \times 10^{-8}$. The value of the second-harmonic tensor element $\chi_{123}(2\omega)$ obtained by Ashkin *et al.*¹⁸ using a He-Ne gas laser operating at 11 520 Å is $(3 \pm 1) \times 10^{-9}$. As the dispersion of $\chi_{312}(2\omega)$ between this wavelength and 6934 Å is presumably small, this value will be used. The first ratio in Eq. (13) is then computed to be $(4.6 \pm 1.4) \times 10^5$.

The numerator of the second ratio cannot be obtained directly from the measurement of Zwicker and Scherrer, as Eq. (11) indicates that the combination $(\chi_{1133}(\omega) - \chi_{3333}(\omega))P_3^2$ is measured. The value of this quantity is 2.62×10^{-4} . As discussed below, it will be assumed that $\chi_{3333}(\omega)$ is much smaller than $\chi_{1133}(\omega)$. The denominator of the second ratio in Eq. (13) is obtained from Fig. 5. The average values of $\chi_{3113}(2\omega)P_3$ at 77°K is $(0.19 \pm 0.06) \times \chi_{312}(2\omega)$. Since $\chi_{3113}(2\omega)P_3$ is determined in terms of $\chi_{312}(2\omega)$, a comparison of the first and second ratios is independent of the numerical value of $\chi_{312}(2\omega)$. The second ratio is $(4.6 \pm 1.6) \times 10^5$. The agreement between the first and second ratios is satisfactory. Similar results are obtained for KD_2PO_4 .

Since second-harmonic generation from $\chi_{3333}(2\omega)$ was not observed, it is not possible to evaluate the third ratio. If the equality is assumed to hold also for the third ratio in Eq. (13), it follows that $\chi_{3333}(\omega)$ is small compared to $\chi_{1133}(\omega)$.

An unexplained result is obtained from Figs. 2 and 5. Below the ferroelectric transition point, the difference between the refractive indices n_1-n_3 becomes smaller, but the second harmonic element $\chi_{311}'(2\omega)$ increases. Similarly, n_2-n_3 becomes larger and $\chi_{322}(2\omega)$ decreases. In the paraelectric phase, n_1-n_3 is positive. From these results and Eqs. (11) and (12) it follows that the ratios $\chi_{123}(\omega)/\chi_{11}(\omega)$ and $\chi_{3113}(2\omega)/\chi_{312}(2\omega)$ must have opposite signs. Similar conclusions apply to the elements $\chi_{113}'(2\omega)$ and $\chi_{223}'(2\omega)$.

The changes in the optical properties of other ferroelectric crystals can also be analyzed in this manner. For example, the symmetry arguments used to determine

¹⁷ D. A. Kleinman, Phys. Rev. **126**, 1977 (1962).

¹⁸ A. Ashkin, G. D. Boyd, and J. M. Dziedzic, Phys. Rev. Letters **11**, 14 (1963).

the allowed linear susceptibility elements of BaTiO_3 in the tetragonal phase indicate that the birefringence is proportional to the square of the polarization. This is observed experimentally.^{19,20} The measurements by Miller¹² of the temperature dependence of the second-harmonic susceptibility indicate that the third-rank tensor elements are linearly proportional to the polarization. A similar dependence is predicted by the theory. As for KH_2PO_4 , there should exist relations between the fourth-rank tensor elements which are responsible for the birefringence and the polarization induced second-harmonic susceptibility. Hofmann²¹ has recently measured the temperature dependence of the refractive index for the ordinary wave. This index does not change at

¹⁹ W. J. Merz, Phys. Rev. **76**, 1221 (1949).

²⁰ H. F. Kay and P. Vousden, Phil. Mag. **40**, 1019 (1949).

²¹ R. Hofmann, Helv. Phys. Acta **35**, 532 (1962).

the transition, indicating that the total birefringence results from a change of n_s . The above theory would then indicate that the relative values of the second-harmonic elements should differ appreciably. Miller's results indicate, however, that the nonlinear tensor elements do not differ by more than a factor 2.5.

Note added in proof. Recently J. E. Geusic, S. K. Kurtz, L. C. Van Uitert, and S. H. Wemple, [Appl. Phys. Letters **4**, 141 (1964)] have measured the electro-optic properties of ABO_3 perovskites in the paraelectric phase at 6328 Å. Their values of the quadratic electro-optic tensor elements of BaTiO_3 , expressed in terms of the static polarization, and the second-harmonic tensor elements of this crystal obtained by Miller¹² are consistent with the theory discussed here to within the experimental accuracy. They are not consistent with Hofmann's data.²¹

Linear Electric Shifts in the Nuclear Quadrupole Interaction in Al_2O_3 *

R. W. DIXON AND N. BLOEMBERGEN

Division of Engineering and Applied Physics, Harvard University, Cambridge, Massachusetts

(Received 23 March 1964)

Electric perturbations of the nuclear magnetic resonances of the Al^{27} nuclei in single-crystal aluminum oxide are discussed. Splittings of the quadrupole satellite resonance lines have been obtained using fields as high as 300 kV/cm. The splittings are caused by equal and opposite changes in the electric-field gradient tensor at crystallographic aluminum sites related to each other by inversion symmetry. Magnitudes and relative signs of the five independent R -tensor elements which completely describe the electrically induced shifts for the C_3 site symmetry of the aluminum nucleus have been determined by applying electric and magnetic fields in various crystallographic directions. These data are compared with similar data obtained earlier from electric shifts in the electron spin resonances of the Cr^{3+} ion in the same crystal.

I. INTRODUCTION

LINEAR electrically induced changes in nuclear and electron spin resonance spectra may exist whenever the site of the interaction lacks inversion symmetry.¹ The first observation of these electrically induced effects was in pure nuclear quadrupole resonance spectroscopy,^{2,3} and several more detailed investigations have since been carried out.⁴⁻⁶ Electric shifts in paramagnetic resonance spectra were first

investigated by Ludwig and Woodbury,⁷ who worked with interstitial transition metal ion impurities in silicon. Artman and Murphy⁸ observed linear shifts in the $m_s = \pm \frac{3}{2} \rightarrow \pm \frac{1}{2}$ transitions of the Cr^{3+} ion in Al_2O_3 for the special case in which the magnetic and electric fields are applied parallel to the crystallographic c axis, and subsequently, Royce and Bloembergen⁹ investigated the complete tensor describing electrically induced shifts in the Cr^{3+} electron-spin resonance spectra in ruby.

Electrically induced splittings in the optical emission spectra of small concentrations of paramagnetic ions in aluminum oxide have also been investigated.¹⁰⁻¹²

* This paper is based on portions of a thesis presented to Harvard University in fulfillment of the thesis requirement for the Ph.D. degree and has been supported by the Joint Services through the U. S. Office of Naval Research Contract 1866(16).

¹ N. Bloembergen, Science **133**, 1363 (1961).

² T. Kushida and K. Saiki, Phys. Rev. Letters **7**, 9 (1961).

³ J. Armstrong, N. Bloembergen, and D. Gill, Phys. Rev. Letters **7**, 11 (1961).

⁴ J. Armstrong, N. Bloembergen, and D. Gill, J. Chem. Phys. **35**, 1132 (1961).

⁵ F. A. Collins, Bull. Am. Phys. Soc. **9**, 25 (1964); thesis, Harvard University (unpublished); Phys. Rev. (to be published).

⁶ R. W. Dixon, Bull. Am. Phys. Soc. **8**, 350 (1963); thesis, Harvard University (unpublished); J. Chem. Phys. (to be published).

⁷ G. W. Ludwig and H. H. Woodbury, Phys. Rev. Letters **7**, 240 (1961).

⁸ J. O. Artman and J. C. Murphy, Bull. Am. Phys. Soc. **7**, 14 (1962).

⁹ E. B. Royce and N. Bloembergen, Phys. Rev. **131**, 1912 (1963).

¹⁰ W. Kaiser, S. Sugano, and D. L. Wood, Phys. Rev. Letters **6**, 605 (1961).

¹¹ M. D. Sturge, Phys. Rev. **133**, A795 (1964).

¹² M. G. Cohen and N. Bloembergen, Bull. Am. Phys. Soc. **9**, 88, (1964). M. G. Cohen, thesis, Harvard University, 1963 (unpublished); M. G. Cohen and N. Bloembergen, Phys. Rev. (to be published).